A Pulse Density Modulation Method for ZVS Full-Bridge Converters in Wireless Power Transfer Systems

Hongchang Li[1], Jingyang Fang[2], Shuxin Chen[2], and Yi Tang[2]
[1]Energy Research Institute
[2]School of Electrical and Electronic Engineering
Nanyang Technological University
Singapore
hongchangli@ntu.edu.sg, yitang@ntu.edu.sg

Kangping Wang
School of Electrical Engineering
Xi'an Jiaotong University
Xi'an, China
wangkangping@stu.xjtu.edu.cn

***Abstract*—This paper aims to combine two advanced techniques, namely, pulse density modulation (PDM) and zero-voltage-switching (ZVS) class-D converters, for wireless power transfer (WPT) systems. PDM enables voltage regulation and efficiency maximization without additional dc/dc stages. ZVS class-D converters ensure soft switching for various coupling and load conditions. However, these two techniques cannot be directly combined because the ZVS relies on the symmetric and continuous switching operation, which would be disrupted by PDM. This paper modifies the topology of the ZVS class-D converter and proposes new operating principles and modulation logics for the modified converter, which is called PDM ZVS full-bridge converter, so that the two techniques are successfully combined. The effectiveness of the proposed method was verified in experiment. The overall efficiency of the experimental WPT system is 94 ~ 72 % when the power transfer distance was 0.1 ~ 0.4 m, while the diameter of the coils was 0.3 m.**

Keywords—maximum efficiency point tracking (MEPT); pulse density modulation (PDM); soft switching; wireless power transfer (WPT).

I. Introduction

The output voltage and efficiency of a wireless power transfer (WPT) system depend on the system's coupling and load conditions [1]. Conventional WPT systems employ maximum efficiency point tracking (MEPT) control strategies to regulate the output voltage and maximize the efficiency by additional dc/dc stages [1-4]. However, the dc/dc stages also generate power losses and increase the complexity of the system. Fortunately, researchers found a more efficient and compact method, i.e., pulse density modulation (PDM) for MEPT, so that the dc/dc stages are no longer needed [5].

The PDM method in [5] is inherently compatible with the dual-side soft switching technique that uses resonant currents to discharge switch output capacitances for zero-voltage-switching (ZVS) [5]. However, this soft switching technique is sensitive to the coupling and load condition of the WPT system. When the coils' coupling is strong or the system's load is light, the magnitudes of resonant currents may not be high enough to fully discharge the switch output capacitance during dead time, and hard switching may occur, resulting in significant switching losses, large voltage spikes, and high-frequency noises. Therefore, the PDM method desires a more robust soft switching technique.

The ZVS class-D converters presented in [6] and [7] are promising to solve the soft switching problem for the PDM. The converters employ ZVS branches to provide independent ZVS currents to discharge switch output capacitances so that the soft switching is not sensitive to operating conditions. However, the ZVS class-D converters are not directly compatible with the original PDM method because the ZVS relies on the symmetric and continuous switching operation, which would be disrupted by PDM.

This paper modifies the topology of the ZVS class-D converter, and more importantly, proposes new operating principles and modulation logics to make the converter compatible with PDM, so that the soft switching problem of PDM WPT systems is resolved. The new converter is called PDM ZVS full-bridge converter.

II. Topology And Principle

Fig. 1 shows the schematic of the main circuit of the proposed PDM ZVS full-bridge converter that operates in inversion mode. The converter is fed by a dc input voltage of magnitude v_{in} and drives a series resonant tank, which has inductance L, capacitance C, and resistance R. The converter is comprised of a conventional full bridge with switches $S_{1\text{-}4}$ and a ZVS branch that consists of a ZVS inductor L_{ZVS} and a dc blocking capacitor C_b. The ZVS branch is connected between the two switching nodes A and B of the two half bridges.

Fig. 2 shows the ideal waveforms when the pulse density d of u_{AB} equals 0.5. As compared with conventional full-bridge converters, some pulses of u_{AB} are removed and the blanks are denoted by "0". The ratio of the number of remaining positive (P) and negative (N) pulses to the total number of P, N and "0" is called pulse density d.

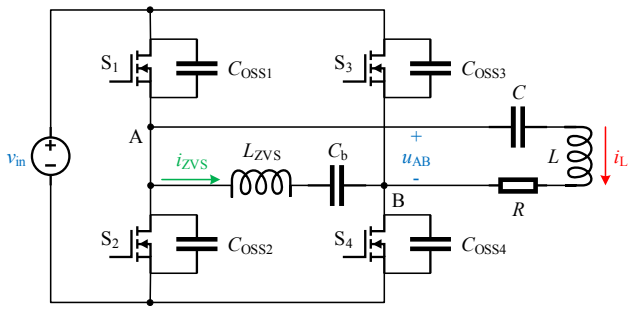

Fig. 1. PDM ZVS full-bridge converter operates in inversion mode.

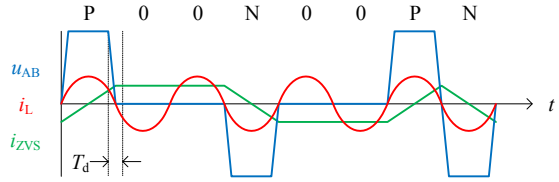

Fig. 2. Ideal waveforms when pulse density $d = 0.5$.

If the switching frequency f_s of the pulses equals the resonant frequency f_r, i.e.

$$f_s = f_r = \frac{1}{2\pi\sqrt{LC}} \tag{1}$$

the resonant current i_L will be in phase with u_{AB}, as shown in Fig. 2. As per the "magnitude-density balance" principle [5], the root-mean-square (RMS) value of the fundamental component of u_{AB} at f_s is

$$U_{AB} = \frac{2\sqrt{2}}{\pi} v_{in} d \ . \tag{2}$$

Therefore, d is the control degree of freedom of the converter.

If C_b is large enough, such that

$$\frac{1}{2\pi\sqrt{L_{ZVS}C_b}} \ll f_s \tag{3}$$

there will be a trapezoid ZVS current i_{ZVS} flowing on the ZVS branch, as shown in Fig. 2. i_{ZVS} increases or decreases linearly during P or N, and holds its peak value during "0"s so that it is always ready for discharging the switch output capacitance at the switching time. The absolute peak value of i_{ZVS} is

$$\left|i_{ZVS\_pk}\right| = \frac{v_{in}}{4 f_s L_{ZVS}} \ . \tag{4}$$

To fully discharge the switch output capacitance during dead time T_d, $|i_{ZVS\_pk}|$ must be large enough and the range of L_{ZVS} is given by

$$L_{ZVS} \le \frac{T_d}{8 f_s C_{OSSQ}} \tag{5}$$

where C_{OSSQ} is the charge equivalent switch output capacitance [6].

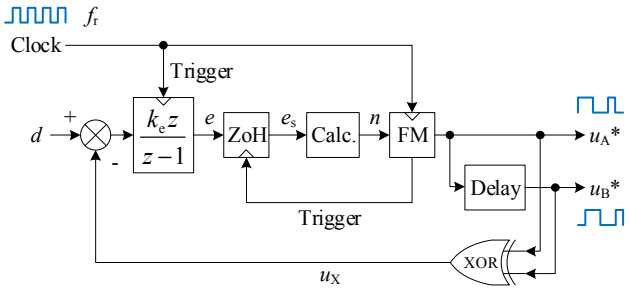

Fig. 3. Schematic of the proposed modulator.

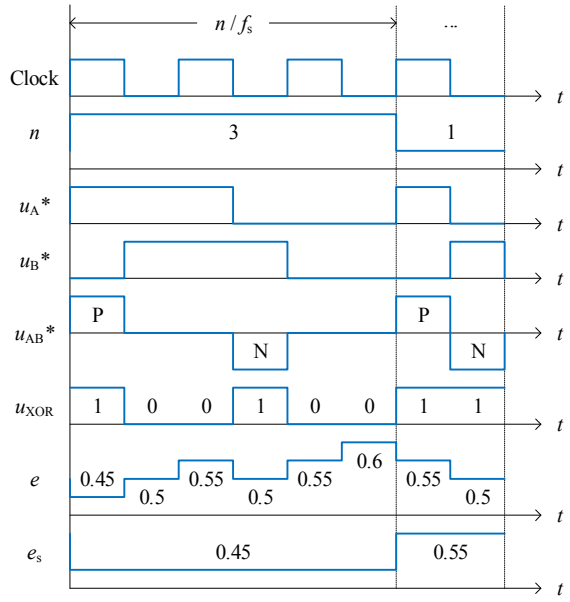

Fig. 4. Ideal waveforms of the proposed modulator when $d = 0.5$.

III. Modulation Method

In order to control the power flow and generate the desired waveforms of i_{ZVS} for any specified d, the P, N and "0" of u_{AB} must follow the four rules:

1) The total density of P and N equals d;
2) P and N are in phase with i_L;
3) P and N occur alternately;
4) P and N are followed by the same number of "0"s.

The 1st and 2nd rules together satisfy the control law of (2). The 2nd rule avoids the back flow of power. The 3rd rule prevents i_{ZVS} from continuously increasing or decreasing when it has reached the peak value. The 4th rule ensures the symmetry of i_{ZVS} so that the absolute values of its positive and negative peaks are equal and both sufficient for the ZVS.

The four rules bring difficulties to the design of the modulator. For example, none of the patterns "P0N0…", "P0…", and "PN00…" is valid for $d = 0.5$ because they violate the 2nd, 3rd, and 4th rules, respectively.

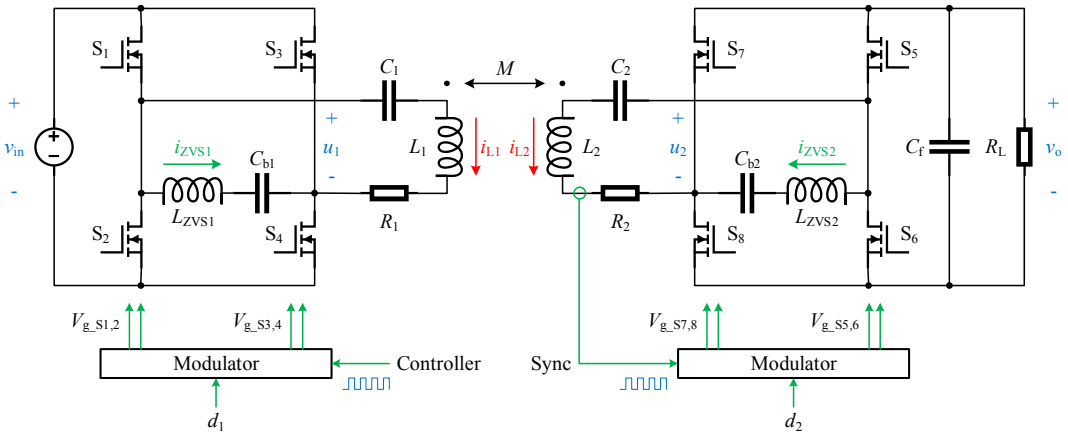

Fig. 5. A WPT system that employs PDM ZVS full-bridge converters on both transmitting and receiving sides.

This paper proposes the modulator shown in Fig. 3 to follow the four rules. The modulator has two input signals. One is a clock signal of a frequency f_s that equals the resonant frequency f_r, and the other one is the specified pulse density d. The output signals are u_A* and u_B*, which are the references for the switching nodes A and B, respectively. The gate drive signals of $S_{1\text{-}4}$ can be generated from u_A* and u_B* by using simple logics that create dead time [8].

The modulator in Fig. 3 operates in two steps. In the first step, a nested frequency modulator "FM" divides the clock frequency by an odd n to generate u_A*, and a delay unit delays u_A* for half a clock cycle to generate u_B*. Fig. 4 shows the waveforms of u_A* and u_B*, as well as their difference u_{AB}* for the cases of $n = 3$ and $n = 1$. It can be verified that u_{AB}* follows the 2nd, 3rd and 4th rules for any odd n. In the second step, n is determined by delta-sigma modulation to follow the 1st rule. The delta-sigma modulation takes the XOR of u_A* and u_B*, which is denoted by u_{XOR}, as the feedback pulses because the pulse density of u_{XOR} equals the total density of the P and N in u_{AB}*. The difference of d and u_{XOR} is accumulated with a gain k_e by a transfer function block, which is triggered by both the rising and falling edges of the clock signal. The accumulation result is denoted by e. e is sampled by a zero-order holder "ZoH" at the end of each frequency modulation period n/f_s. The sampled e is denoted by e_s. n is derived from e_s by the block "Calc." in terms of

$$n = 2\left\lceil \frac{0.5}{\max\left(e_s, e_{\min}\right)} \right\rceil - 1 \tag{6}$$

where $e_{min} > 0$ is a lower limit on e_s. A typical value of e_{min} is 0.2, and $k_e = 0.1$ is appropriate for such an e_{min}.

IV. The WPT System

Fig. 5 shows a WPT system that employs PDM ZVS full-bridge converters on both transmitting and receiving sides as inverter and rectifier, respectively. The inverter converts the input dc voltage v_{in} to its switching node voltage u_1 and injects energy into the transmitting side resonator, which has inductance L_1, capacitance C_1, and equivalent series resistance (ESR) R_1. The resonant current on the transmitting side is denoted by i_{L1}. Symmetrically, the rectifier converts the output dc voltage v_o to its switching node voltage u_2 and absorbs energy from the receiving side resonator, which has inductance L_2, capacitance C_2, and ESR R_2. The resonant current on the receiving side is denoted by i_{L2}. In addition, the mutual inductance between L_1 and L_2 is M, the filter capacitance is C_f, and the load resistance is R_L.

The transmitting side modulator modulates u_1 using an independent clock signal and a specified pulse density d_1. The RMS value of the fundamental component of u_1 is

$$U_1 = \frac{2\sqrt{2}}{\pi} v_{in} d_1 \tag{7}$$

The receiving side modulator modulates u_2 using the pulses synchronized with i_{L2} and a specified pulse density d_2. The RMS value of the fundamental component of u_2 is

$$U_2 = \frac{2\sqrt{2}}{\pi} v_o d_2 \tag{8}$$

Under fully tuned condition, namely

$$\omega_s = \frac{1}{\sqrt{L_1 C_1}} = \frac{1}{\sqrt{L_2 C_2}} \tag{9}$$

where ω_s is the angular frequency of the clock signal, the system's steady state operating point is given by

$$\begin{cases} I_{L1} = \dfrac{2\sqrt{2} v_{in} d_1}{\pi\left(R_1 + R_r\right)} \\ I_{L2} = \dfrac{\omega_s M}{R_2 + R_e} I_{L1} \\ v_o = \dfrac{2\sqrt{2}}{\pi} d_2 I_{L2} R_L \end{cases} \tag{10}$$

where R_e is the ac equivalent load resistance:

$$R_e = \frac{8}{\pi^2} {d_2}^2 R_L \tag{11}$$

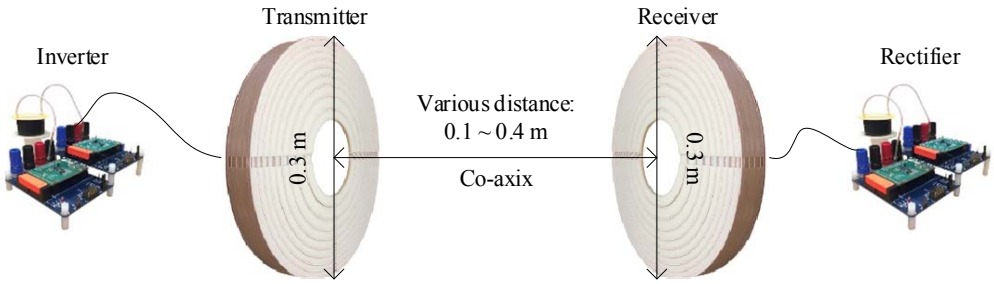

Fig. 6. Spatial configuration of the WPT system.

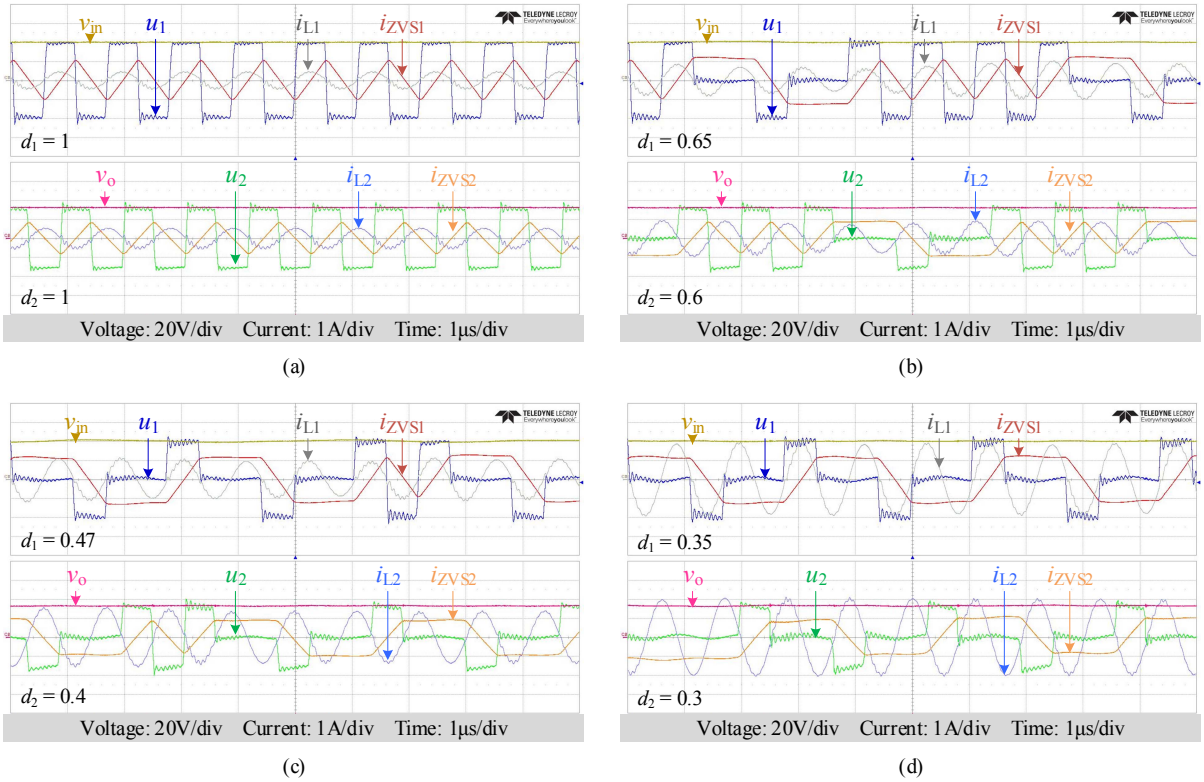

Fig. 7. Operating waveforms of the WPT system when the power transfer distance is (a) 0.1 m, (b) 0.2 m, (c) 0.3 m, and (d) 0.4 m.

and R_r is the reflected resistance:

$$R_r = \frac{(\omega_s M)^2}{R_2 + R_e} \tag{12}$$

Since the system provides two control degrees of freedom, i.e. d_1 and d_2, the MEPT control can be adopted by using d_2 to optimize R_e and d_1 to regulate v_o [5].

V. Experiment

A WPT system prototype as described in Fig. 5 was built using two PDM ZVS full-bridge converters along with a pair of resonant tanks [5]. The spatial configuration of the system is shown in Fig. 6. The parameters are listed in Table I. The input voltage of the inverter was fixed at 40 V. The load resistance was fixed at 100 Ω. This resistance was selected because such a large resistance results in low resonant currents and output power. Low resonant currents usually challenge the soft switching of existing WPT systems. And low output power usually results in low efficiency. The test with 100 Ω load resistance was actually the "worst-case test" of the system.

Experiment was carried out at various power transfer distances, 0.1 ~ 0.4 m, while the MEPT control was manually adopted by adjusting the pulse densities d_1 and d_2 so that the system maintained a nearly constant output voltage, 32.5 V, and achieved the maximum overall efficiency, 94 ~ 72 %. Fig. 7 shows the measured operating waveforms, which indicate that the system operated as expected. Fig. 8 shows the output voltage and overall efficiency, which verify the effectiveness of voltage regulation and efficiency maximization.

TABLE I PARAMETERS OF THE WPT PROTOTYPE

Symbol	Quantity	Value
T_d	Dead time	50 ns
L_{ZVS}	ZVS inductance	10 μH
C_b	Dc blocking capacitance	1 μF
$L_{1,2}$	Resonant inductance	76.6 μH
$C_{1,2}$	Resonant capacitance	400 pF
$f_{r1,2}$	Resonant frequency	0.909 MHz

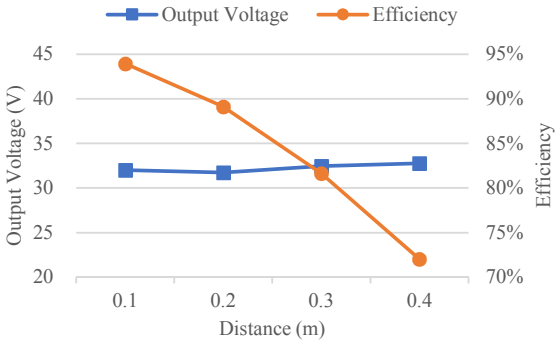

Fig. 8. Effects of voltage regulation and efficiency maximization.

VI. COMPARISON TO REPORTED WPT SYSTEMS

Table II compares the WPT prototype in this paper to the representative reported WPT systems. All these systems have the function of MEPT (but may have a different name, e.g., MET or MEET). The key parameters, including coil diameter, power transfer distance, and overall efficiency are listed in the table. (The overall efficiency is the source-to-load efficiency including power converters.)

Fig. 9 shows the efficiency with respect to the distance ratio, which is defined as power transfer distance over coil diameter. The distance ratio is considered because it is the major limiting factor on the efficiency. It can be seen from Fig. 9 that for any of the WPT systems, the higher distance ratio, the lower efficiency can be achieved, even with MEPT. However, in comparison to other WPT systems, the prototype in this paper achieved higher efficiency with the same distance ratio, and higher distance ratio for the same efficiency.

VII. CONCLUSION

PDM is successfully adopted in ZVS full-bridge converters by using the proposed operating principles and modulation logics. The effectiveness of the proposed method is verified by an experimental WPT system that employs PDM ZVS full-bridge converters on both transmitting and receiving sides. The system can maximize the efficiency and regulate the output voltage simultaneously, while maintaining soft switching at various operating conditions. As compared with reported WPT systems, the system in this paper achieved much higher efficiency in a wide range of power transfer distance, among which higher than 80 % overall efficiency was observed when the distance equaled the coils' diameter.

TABLE II REPORTED WPT SYSTEMS WITH MEPT

#	Coil diameter (mm)	Distance (mm)	Efficiency (%)	Reference
1	270	100	87	[1]
		150	83	
		200	79	
		250	74	
2	600	100	96	[9]
		135	94	
		170	92	
3	100	40	72	[10]
4	43	23	73	[11]
		28	66	
		33	58	
5	88	25	89	[4]
		33	87	
6	310	200	73	[12]
7	300	500	70	[5]
8	300	100	94	This paper
		200	89	
		300	82	
		400	72	

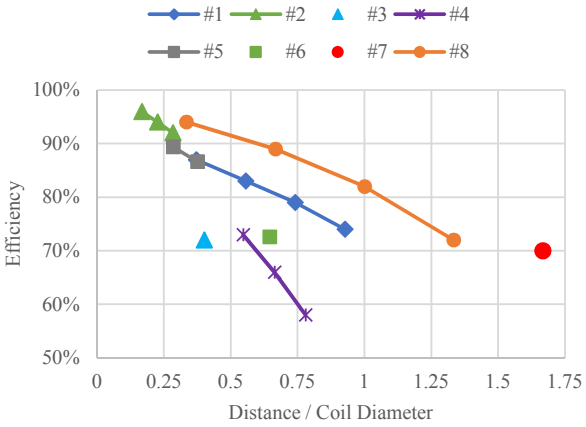

Fig. 9. Efficiency comparison of the WPT systems listed in Table II.

REFERENCES

[1] H. Li, J. Li, K. Wang, W. Chen, and X. Yang, "A Maximum Efficiency Point Tracking Control Scheme for Wireless Power Transfer Systems Using Magnetic Resonant Coupling," *IEEE Transactions on Power Electronics*, vol. 30, no. 7, pp. 3998-4008, 2015.

[2] T. D. Yeo, D. Kwon, S. T. Khang, and J. W. Yu, "Design of Maximum Efficiency Tracking Control Scheme for Closed-Loop Wireless Power Charging System Employing Series Resonant Tank," *IEEE Transactions on Power Electronics*, vol. 32, no. 1, pp. 471-478, 2017.

[3] X. Dai, X. Li, Y. Li, and P. Hu, "Maximum Efficiency Tracking for Wireless Power Transfer Systems with Dynamic Coupling Coefficient Estimation," *IEEE Transactions on Power Electronics*, 2017. (Published online.)

[4] Z. Huang, S. C. Wong, and C. K. Tse, "Control Design for Optimizing Efficiency in Inductive Power Transfer Systems," *IEEE Transactions on Power Electronics*, 2017. (Published online.)

[5] H. Li, J. Fang, S. Chen, K. Wang, and Y. Tang, "Pulse Density Modulation for Maximum Efficiency Point Tracking of Wireless Power Transfer Systems," *IEEE Transactions on Power Electronics*, 2017. (Published online.)

[6] M. A. d. Rooij, "The ZVS voltage-mode class-D amplifier, an eGaN FET-enabled topology for highly resonant wireless energy transfer," in *2015 IEEE Applied Power Electronics Conference and Exposition (APEC)*, 2015, pp. 1608-1613.

[7] M. d. Rooij and Y. Zhang, "eGaN FET based 6.78 MHz Differential-Mode ZVS Class D AirFuel Class 4 Wireless Power Amplifier," in *PCIM Europe 2016; International Exhibition and Conference for Power Electronics, Intelligent Motion, Renewable Energy and Energy Management*, 2016, pp. 1-8.

[8] EPC Corporation, "Development Board EPC9003C Quick Start Guide," 3rd ed. El Segundo, CA, USA.

[9] T. Diekhans and R. W. De Doncker, "A Dual-Side Controlled Inductive Power Transfer System Optimized for Large Coupling Factor Variations and Partial Load," *IEEE Transactions on Power Electronics*, vol. 30, no. 11, pp. 6320-6328, 2015

[10] M. Fu, H. Yin, M. Liu, and C. Ma, "Loading and Power Control for a High-Efficiency Class E PA-Driven Megahertz WPT System," *IEEE Transactions on Industrial Electronics*, vol. 63, no. 11, pp. 6867-6876, 2016.

[11] X. Tang, J. Zeng, K. P. Pun, S. Mai, C. Zhang, and Z. Wang, "Low-cost Maximum Efficiency Tracking Method for Wireless Power Transfer Systems," *IEEE Transactions on Power Electronics*, 2017. (Published online.)

[12] W. Zhong and S. Y. R. Hui, "Maximum Energy Efficiency Operation of Series-Series Resonant Wireless Power Transfer Systems Using On-Off Keying Modulation," *IEEE Transactions on Power Electronics*, 2017. (Published online.)